Micron 166 (2023) 103412

Contents lists available at ScienceDirect

Micron

journal homepage: www.elsevier.com/locate/micron

The sperm structure of the diving beetles Stictonectes optatus (Seidlitz, 1887) and Scarodytes halensis (Fabricius, 1787) (Dytiscidae, Hydroporinae) with evidence of a spermatostyle in the sperm conjugation.

David Mercati, Pietro Paolo Fanciulli, Pietro Lupetti, Romano Dallai *

Department of Life Sciences, University of Siena, Italy

ARTICLE INFO

Keywords:
Dytiscidae-Hydroporinae sperm structure
Sperm conjugation
Spermatostyle

ABSTRACT

The structure of the male genital organs and spermiogenesis of two diving beetles, *Stictonectes optatus* and *Scarodytes halensis* were studied for the first time. *S. optatus* shows unifollicular testes consisting of a long tubule apically forming a globular structure. The deferent duct epithelia show a secretory activity involved in the spermatostyle organization. They are connected with two very large accessory glands. *Sc. halensis* has a more common structure of the male genital apparatus with unifollicular cylindrical testes and very long deferent ducts. *Sc. halensis* accessory glands are smaller than those of *S. optatus*. The sperm structure in both species is characterized by a small acrosome, a flattened nucleus with a lateral extension containing a centriole from which a long flagellum originates. Both species exhibit sperm conjugation with long sperm bundles showing nuclei orderly arranged in sperm-heads stacks and free flagella. In addition, *S. optatus* has a thick layer of secretion surrounds these sperm-head stacks. Such a secretion is considered a spermatostyle. This finding represents the first record about the presence of this structure among Dytiscidae. In the flagellum, a typical axoneme with a 9 + 9 + 2 microtubular complex, and two mitochondrial derivatives are present in both species. Those of *S. optatus* have a peculiar shape with the apical side, in cross-section, displaying pointed corners. Two small accessory bodies are located between the axoneme and the two mitochondrial derivatives.

1. Introduction

Postcopulatory sexual selection is considered the main agent determining the sperm characteristics in animal reproduction. This hypothesis was confirmed in different organisms, insects included (Stockley et al., 1997; Jamieson et al., 1999; Birkhead, 2000; Miller and Pitnick, 2002; Pitnick et al., 2009; Pizzari and Parker, 2009). The consequence of postcopulatory sexual selection is the production of sperm with a great diversification in their length, general shape and sperm conjugation. Sperm conjugation is the physical aggregation of two or more sperm cells favouring the transport to the female reproductive tract (Ballowitz, 1895).

The aggregation types detected so far are distinct according to their origin. The primary type is formed during spermatogenesis with sperm cells in each aggregate originating from the same spermatogonia, which remain grouped after the completion of cell individualization process. The secondary type occurs when isolated sperm cells, even from different cysts, are grouped later in the vasa deferentia (Pitnick et al., 2009; Higginson and Pitnick, 2011; Salazar et al., 2022). Secondary sperm aggregation can occur by diverse mechanisms giving varied morphological forms: a) sperm bundle or individualized sperm attached by the head to a rod of extracellular material (the spermatostyle) as it occurs in Gyrinidae and in some Carabidae (Breland and Simmons, 1970; Dallai et al., 2019, 2020; Salazar et al., 2022) or with the heads embedded in a dense extracellular material (the spermatostyle) as in other Carabidae (Dallai et al., 2019, 2020); b) sperm pairing when two sperm heads are united by their ventral side in an antiparallel fashion. Intramembrane particles and a specialized type of glycocalyx containing granules were observed between the paired sperm heads in Dytiscidae (Ballowitz, 1895; Dallai and Afzelius, 1985, 1987; Mackie and Walker, 1974; Werner, 1976); c) sperm rouleaux, when the tip of a sperm head slips into another sperm head to form an ordered stack with the perfect shape of two closely adherent sperm (Higginson and Pitnick, 2011; Salazar et al., 2022). No spermatostyle was assumed to be present in the

* Corresponding author.
E-mail addresses: david.mercati@unisi.it (D. Mercati), paolo.fanciulli@unisi.it (P.P. Fanciulli), pietro.lupetti@unisi.it (P. Lupetti), romano.dallai@unisi.it (R. Dallai).

https://doi.org/10.1016/j.micron.2023.103412
Received 4 October 2022; Received in revised form 19 December 2022; Accepted 2 January 2023
Available online 5 January 2023

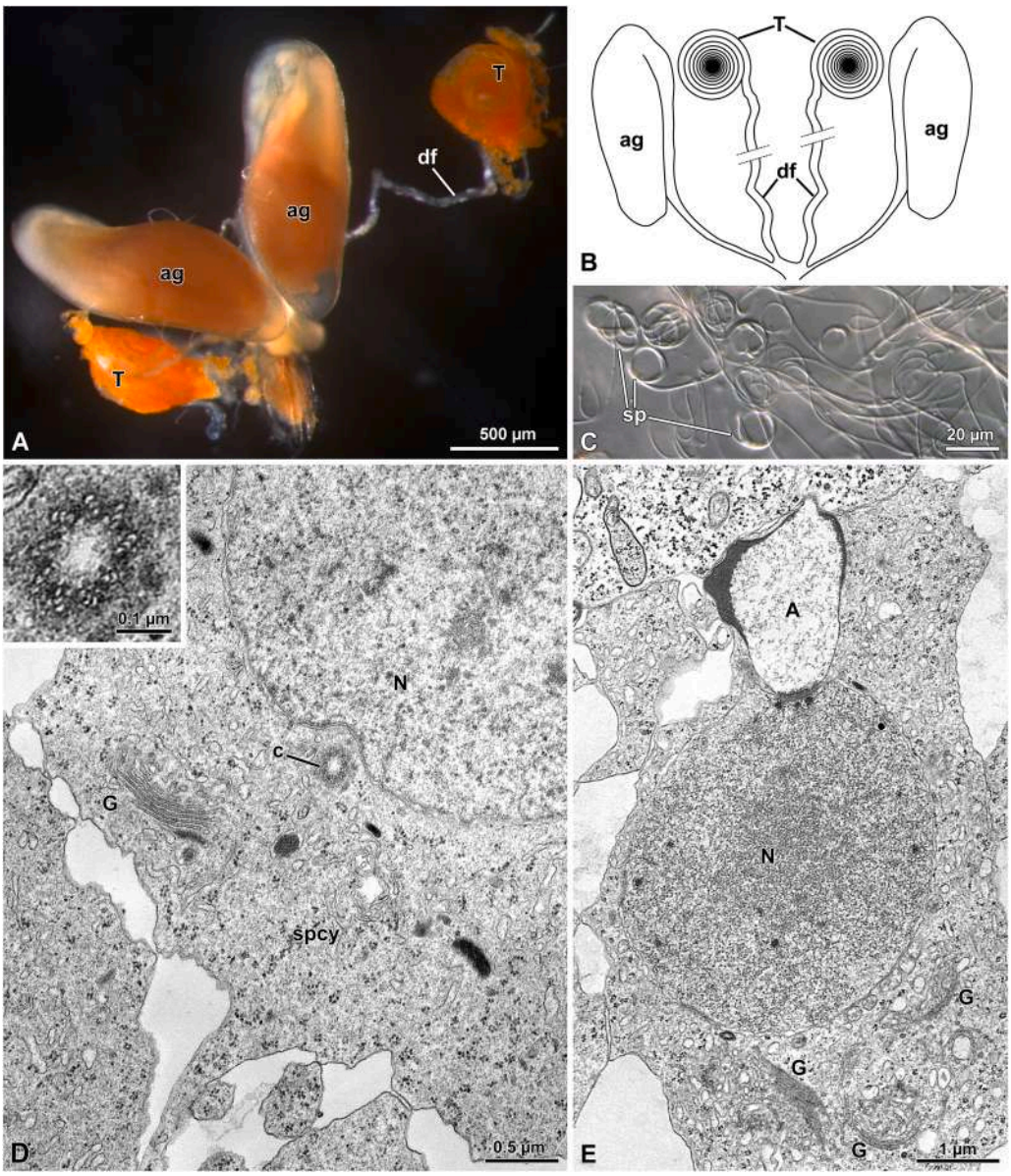

Fig. 1. Stictonectes optatus. A - Light microscopic view of the male genital organs showing the apical globular unifollicular testes, surrounded by yellow fat body, the deferent duct and the large accessory glands. B - Schematic drawing of the general organization of the male genital organs. C - Free sperm taken from a female spermatheca, forming numerous spirals. D - Cross section through the apical globular testes to show a spermatocyte. Note the large nucleus, the typical centriole and the Golgi apparatus. In the inset, detail of the centriole with the microtubule triplets. E - Cross section of early spermatid with the ovoidal nucleus and the apical acrosome. In the cytoplasm, some Golgi apparatuses are visible. A, acrosome; ag, accessory glands; c, centriole; df, deferent ducts; G, Golgi apparatus; N, nucleus; sp, spermatozoa; spcy, spermatocyte; T, testes.

diving beetles (Dytiscidae), a taxon with more than 4500 species worldwide (Nilsson, 2001; Miller, 2001, 2003; Nilsson and Fery, 2006; Beutel et al., 2020) that shows either singleton sperm, sperm aggregation and sperm conjugation with sperm joining by secretory material. Such peculiar array is retained to help motility or transport through the female reproductive tract (Higginson and Pitnick, 2011; Higginson et al., 2012).

Accurate studies of sperm ultrastructure, reveal a series of important features useful for a comparative analysis of the different groups of Adephaga (Werner, 1976; Carcupino et al., 2002; Dallai and Afzelius, 1985, 1987; Hodgson et al., 2013; Dallai et al., 2019, 2020; Gomez and Maddison, 2020; Gomez et al., 2023).

The sperm ultrastructure of Dytiscidae is known for few species (Ballowitz, 1895; Mackie and Walker, 1974; Werner, 1976; Dallai and Afzelius, 1985, 1987). These works have pointed out that different species of Dytiscinae and Colymbetinae subfamilies exhibit either single or multiple sperm grouped with different modalities, a characteristic shared with other Adephaga such as Gyrinidae and Carabidae (Dallai et al., 2019, 2020; Gomez and Maddison, 2020; Salazar et al., 2022; Gomez et al., 2023).

Ultrastructural data are still missing for the subfamily Hydroporinae. Here we aim to cover this gap with a study on the sperm ultrastructure of two small-sized species, *S. optatus* and *Sc. halensis*.

2. Materials and methods

2.1. Specimens

Males of *Stictonectes optatus* and *Scarodytes halensis* were collected in a small creek near Grosseto, Italy on June 6, 15, 22, and October 10, 2022. The species were determined by Dr Saverio Rocchi of the Museum "La Specola", Florence, and preserved in the collection of the specialist.

S. optatus is a small Hydroporinae distributed in the West-Europe; *Sc. halensis* is a little bit larger species with a larger geographic distribution, recorded in Europe and North-Africa. Both species belong to the tribe Hydroporini and to two different subtribes (Miller and Bergsten, 2016).

2.2. Light microscopy

After dissection of both species in 0.1 M pH 7.2 phosphate buffer (PB) to which 3% of sucrose was previously added, male genital organs were removed and the whole systems were photographed with an Olympus

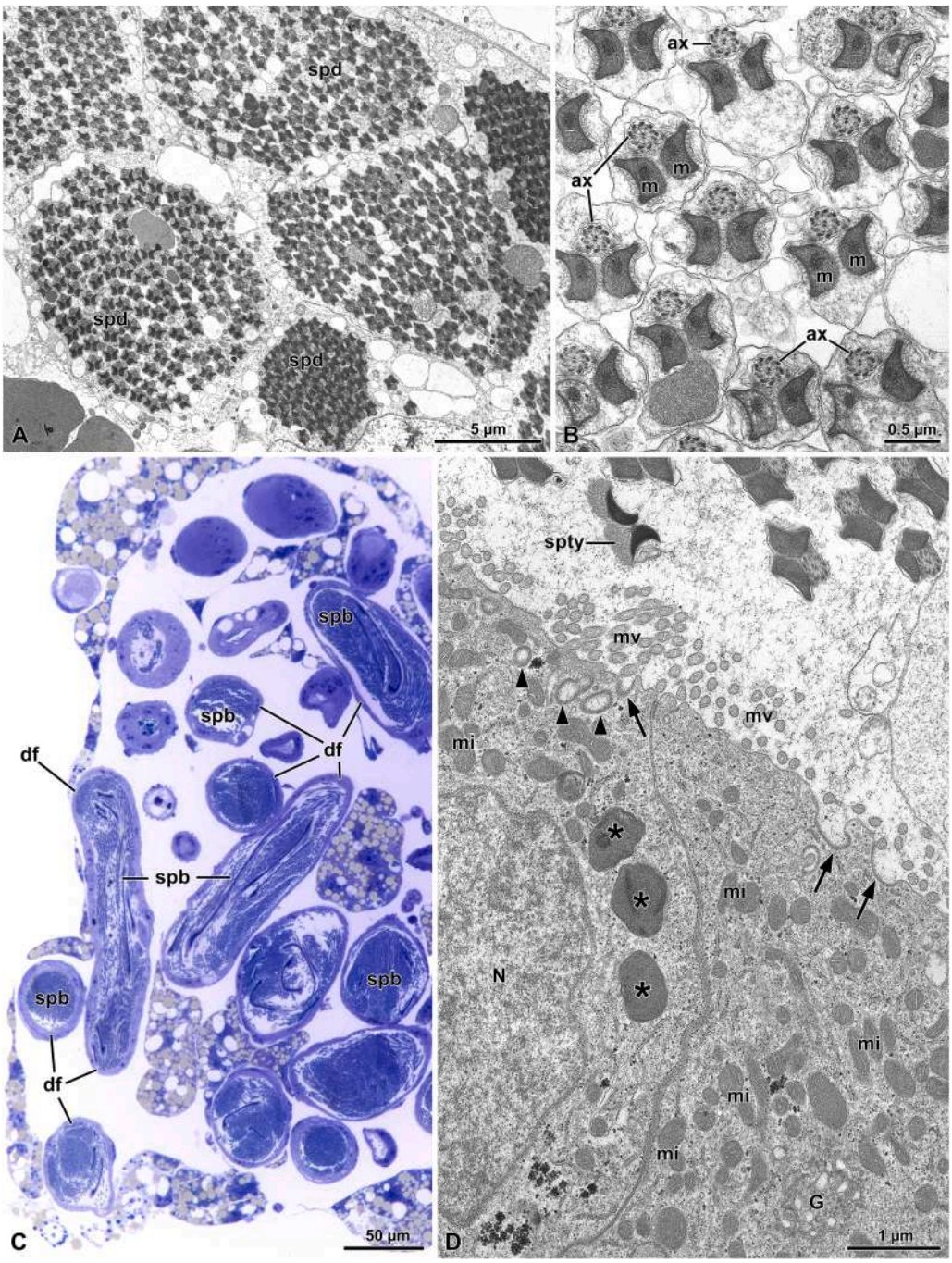

Fig. 3. S. optatus. A - Cross section through the apical follicle showing the lumen filled with spermatid cysts. B - Cross section of a cyst of spermatid flagella with their axonemes and mitochondrial derivatives. C - Semithin section of the deferent duct. Note the duct lumen filled with sperm bundles with long sperm-heads stacks surrounded by spermatostyles. D - Cross section through the deferent duct wall showing the nucleus, the numerous mitochondria, the apical microvilli and some short cisterns of rough endoplasmic reticulum. Note the large masses of dense material (asterisks) and the vesicles (arrowheads) close to the apical plasma membrane. Some of them open and flow their secretion in the duct lumen (arrows).
ax; axoneme; df, deferent duct; m, mitochondrial derivatives; mi, mitochondria; mv, microvilli; N, nucleus; spb, sperm bundles; spd, spermatid; spty, spermatostyle.

SZX12 stereomicroscope equipped with an AxioCam MRC5 HR camera (Carl Zeiss). Bundles and free sperm were picked out from deferent ducts of males of the two species and observed and photographed with a Leica DMRB light microscope equipped with an AxioCam MRC5 HR camera (Carl Zeiss. Free sperm of *S. optatus* were also taken from a female spermatheca. In order to visualize the sperm nucleus, part of these samples were stained for DNA by adding a drop of 1 µg/mL of Hoechst 33258 dye in 0.1 M PB.

2.3. Light microscopy of semithin sections

Part of the material dissected from both species was fixed overnight in 3% glutaraldehyde in PB. After rinsing in PB, the material was post-fixed in 1% osmium tetroxide in PB for 2 h. After thorough rinsing, the material was dehydrated with a graded series of alcohols (50–100%), then transferred to propylene oxide and finally embedded into an Epon-araldite resin mixture. After resin polymerization for 48 h at 60 °C, semithin sections were obtained with a Reichert Ultracut ultramicrotome. Sections were then stained with 1% toluidine blue, observed and photographed with a Leica DMRB epifluorescence-interference light microscope equipped with an AxioCam MRC5 HR (Carl Zeiss) camera.

2.4. Transmission electron microscopy

Ultrathin sections for transmission electron microscopy were cut with an ultramicrotome Reichert Ultracut from embedded samples of both species. Sections were stained routinely with uranyl acetate and lead citrate, and finally observed with a Philips CM 10 Transmission

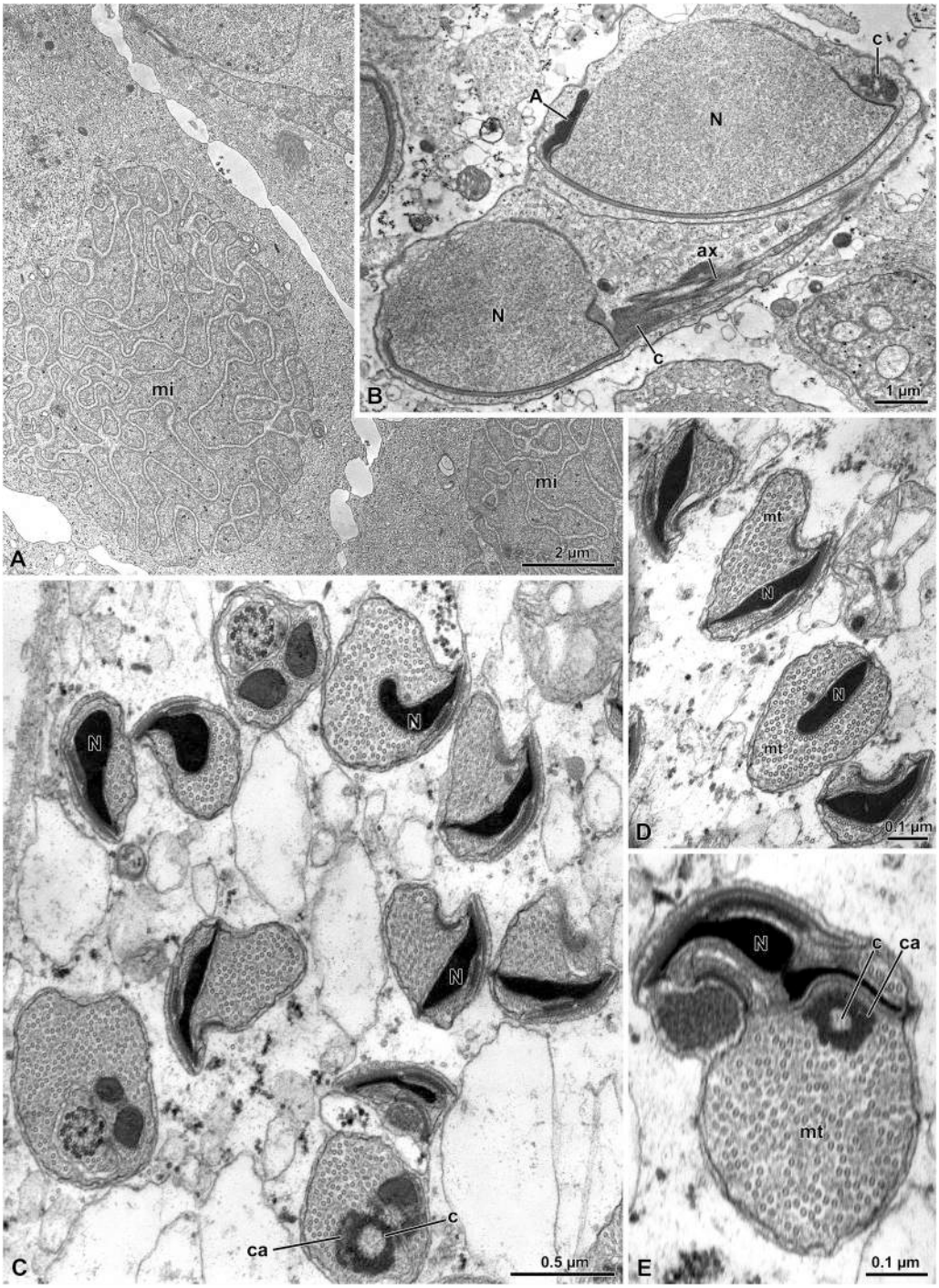

Fig. 2. S. optatus. A - Cross section of early spermatid with mitochondria forming "nebenkern". B - Longitudinal section of two elliptical spermatid nuclei with the apical flattened acrosome and the centriole on the opposite side. A long axoneme is starting from this region. C - Cross section of the end of the thin nuclear region with the centriole surrounded by the centriole adjunct material. Note the numerous microtubules in the residual cytoplasm. D, E - Cross section of the laminar nuclei. In the residual cytoplasm, numerous microtubules are visible.
A, acrosome; ax, axoneme; c, centriole; ca, centriole adjunct material; mi, mitochondria; mt, microtubules; N, nucleus.

electron microscope operating at an electron accelerating voltage of 80 kV.

2.5. Scanning electron microscopy

Bundles and free spermatozoa of *Sc. halensis* isolated after dissection, were transferred onto 1% Poly-L-lysine pre-treated glass cover slips and fixed for 1 h with 1% osmium tetroxide solution in distilled water. The samples were rinsed in distilled water and dehydrated in alcohol prior to critical point drying in a Balzer's CDP 010. The material was mounted on aluminium stubs, coated with gold using a Balzer's Med 010 sputtering device and examined using a Philips XL30 Scanning electron microscope operating at an electron accelerating voltage of 15 kV.

3. Results

3.1. Stictonectes optatus

3.1.1. The male genital system

The male genital system of *S. optatus* consists of two monofollicular testes surrounded by yellow fat body (Fig. 1A). Each testis is a coiling duct, 10–20 µm wide, which gives it a globular appearance, 300–500 µm wide, in the apical region (Fig. 1A, B). Testes continue with long deferent ducts, 1.0 mm long and 50–120 µm wide, according to the sectioning level. These ducts open into the proximal end of very large accessory glands, 1.6 mm long and 0.6 mm wide (Fig. 1A, B), which is extended anteriorly, partially hiding the deferent ducts. The accessory

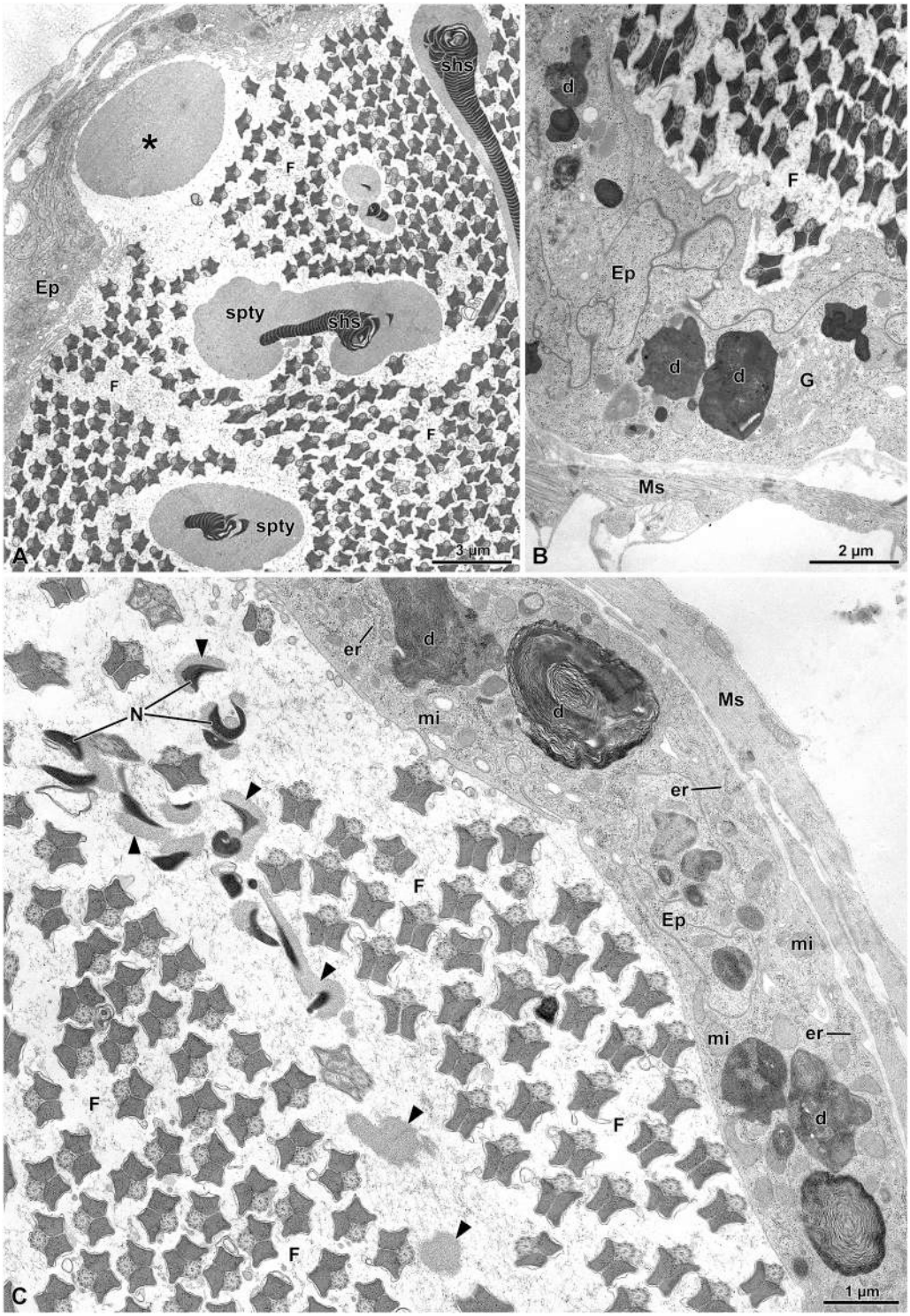

Fig. 4. S. optatus. A - Cross section of the deferent duct with the lumen showing sperm-head stacks and many flagella. Note the large masses of secretion (asterisk), with spermatostyles showing a moderated electron-dense content, surrounding the sperm stacks. B - Cross section through the deferent duct epithelium with several dense masses of secretion and a Golgi apparatus. Beneath the epithelium a thin layer of muscle fibers is visible. C - Cross section of the deferent duct. In the lumen, many flagella are visible together with some isolated nuclei, surrounded by a secretion similar to that of the spermatostyle (arrowheads). In the cytoplasm, several dense masses of variable size, mitochondria and short cisterns of rough endoplasmic reticulum are visible. Beneath the epithelium, a layer of muscle fibers is present.
d, dense masses of secretion; Ep, epithelium; er, endoplasmic reticulum; F, flagella; G, Golgi apparatus; mi, mitochondria; Ms, muscle fibers; N, nucleus; shs, sperm-head stacks; spty; spermatostyle.

glands flow into a common ejaculatory duct.

3.1.2. *Spermatogenesis*

The spermatogenesis occurs in the apical region of the testes. Cross-sections through this region of follicle testis, show several germ cysts at different stage of development. Each cyst contains 128 cells, as a result of 2^7 cell divisions (Fig. 3A). Spermatocytes are large cells displaying conventional features with large nucleus hosting uncondensed chromatin; in the cytoplasm of these cells, a typical centriole with microtubular triplets, and a Golgi apparatus are present (Fig. 1D). In the spermatids, mitochondria assemble to form “nebenkern” (Fig. 2B), which are visible as two large complexes about 6.6 µm wide. Along their maturation, spermatids progressively modify their appearance. A thin acrosome (1.5 µm wide) is positioned at the anterior apical end of the nucleus (Fig. 1E). The nuclei, at the initial stage, have an elliptical shape, 6.5 µm long and 3.5 µm wide (Fig. 1E), but further they become dense and acquire a flattened shape with a thickening at their central region (Fig. 2B-E). The flagellar axoneme starts from a centriole (Fig. 2C, E) which is made of a complex of nine microtubular doublets, without dynein arms, and accessory tubules. A scarse dense centriole adjunct

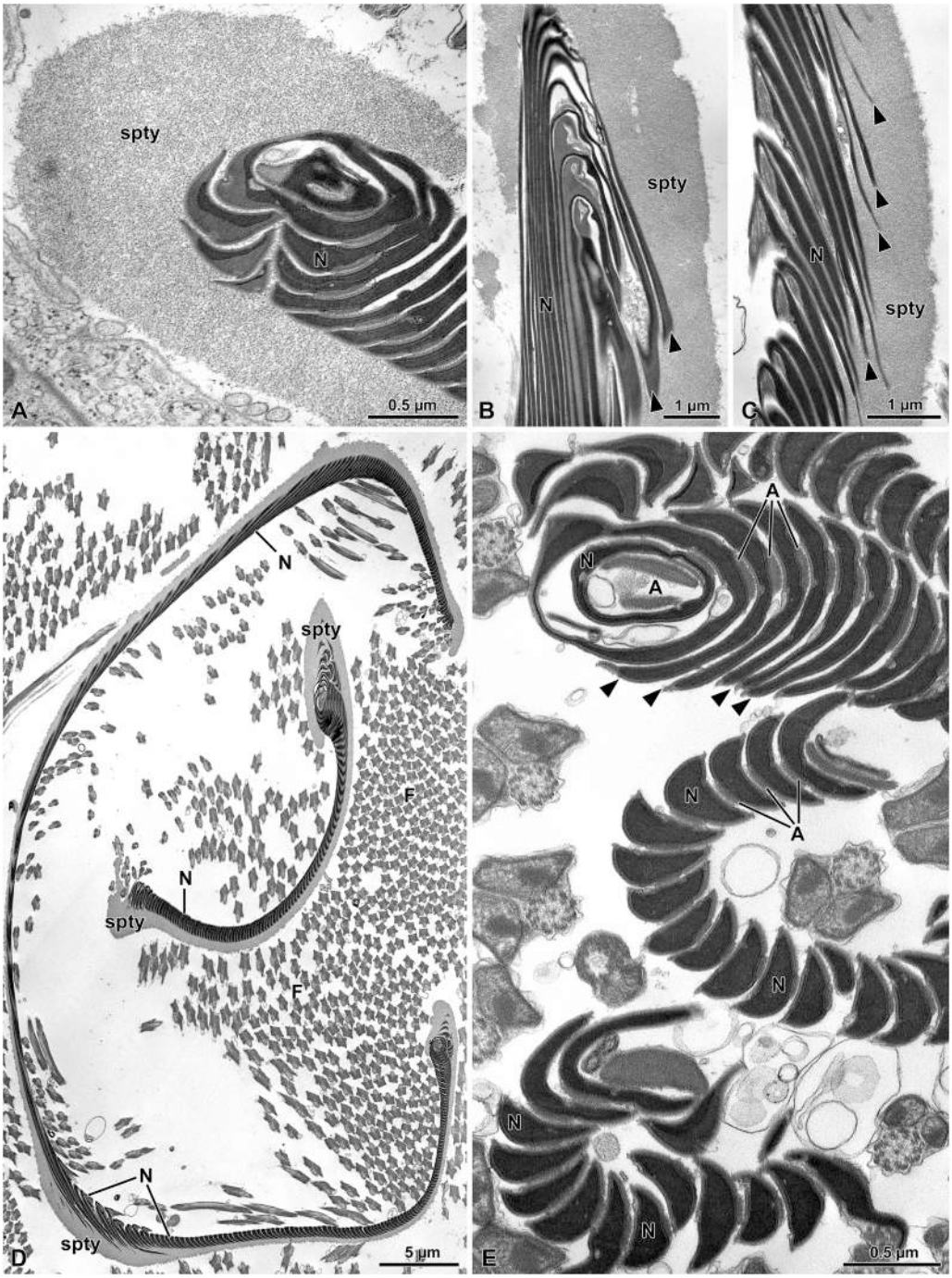

Fig. 6. S. optatus. A, B, C, D - Cross and longitudinal sections of long chains of sperm-heads and flagella. Note how the first nuclei of the chain are positioned to allow a perfect insertion of the following sperm head. Note also that each sperm nucleus prolongs backward with a thin lamina (arrowheads). The sperm-heads are surrounded by electron-dense material of the spermatostyle. E - Cross section through the posterior end of the deferent duct showing long sperm–head chains broken into several parts. Note that the spermatostyle around the sperm nuclei is lacking. The micrograph allows to see well how the first sperm-head is adapted to allow the insertion of the following nuclei Note also the short acrosome on the dorsal nuclear region. A, acrosome; F, flagella; N, nuclei; spty, spermatostyle.

material surrounds the microtubular complex (Fig. 2E). The thin cytoplasm surrounding these structures is filled with microtubules (Fig. 2C-E). The flagellar axoneme is flanked by two cylindrical mitochondrial derivatives, in cross-section, with a central region showing a dense and compact material (Fig. 3B).

3.1.3. *Sperm ultrastructure*

A cross section through the deferent duct shows several sperm complexes in their lumen (Fig. 3C). The epithelial wall in this duct is 3.2–6.0 µm high, formed by cells provided with an elliptical nucleus (9.2 µm X 1.5 µm) and cytoplasm rich in mitochondria, some Golgi apparatuses and a few cisterns of rough endoplasmic reticulum (Fig. 3D). Large masses of dense material, 1.2–1.5 µm wide, of variable size and shape, and secretory vesicles are visible in the cytoplasm (Figs. 3D; 4B, C). Some of these vesicles contact the apical plasma membrane, fuse with it and flow their secretion into the deferent duct lumen (Fig. 3D). The secretion has a moderated electron-density and often it adheres to or embeds isolated sperm nuclei (Fig. 4C). Such material apparently has the same electron-density of that surrounding the sperm-head stacks present in the deferent duct lumen (Fig. 4A).

The sperm of *S. optatus* are about 0.9 mm long (Fig. 1C). In the thin deferent duct, sperm cells are aggregated to form long chains of more than hundred units with their heads aligned in register (Figs. 3C; 5A, B; 6A-D). The nuclei have a semilunar shape showing a thicker central part that reach 0.15–0.16 µm of thickness in cross-section (Fig. 6A-C, E). Instead, the two lateral regions are very flat, only 82–85 nm thick (Fig. 6B, C). On the dorsal side of the thickened region, an electron-dense material, sometimes with an irregular shape, is visible. This

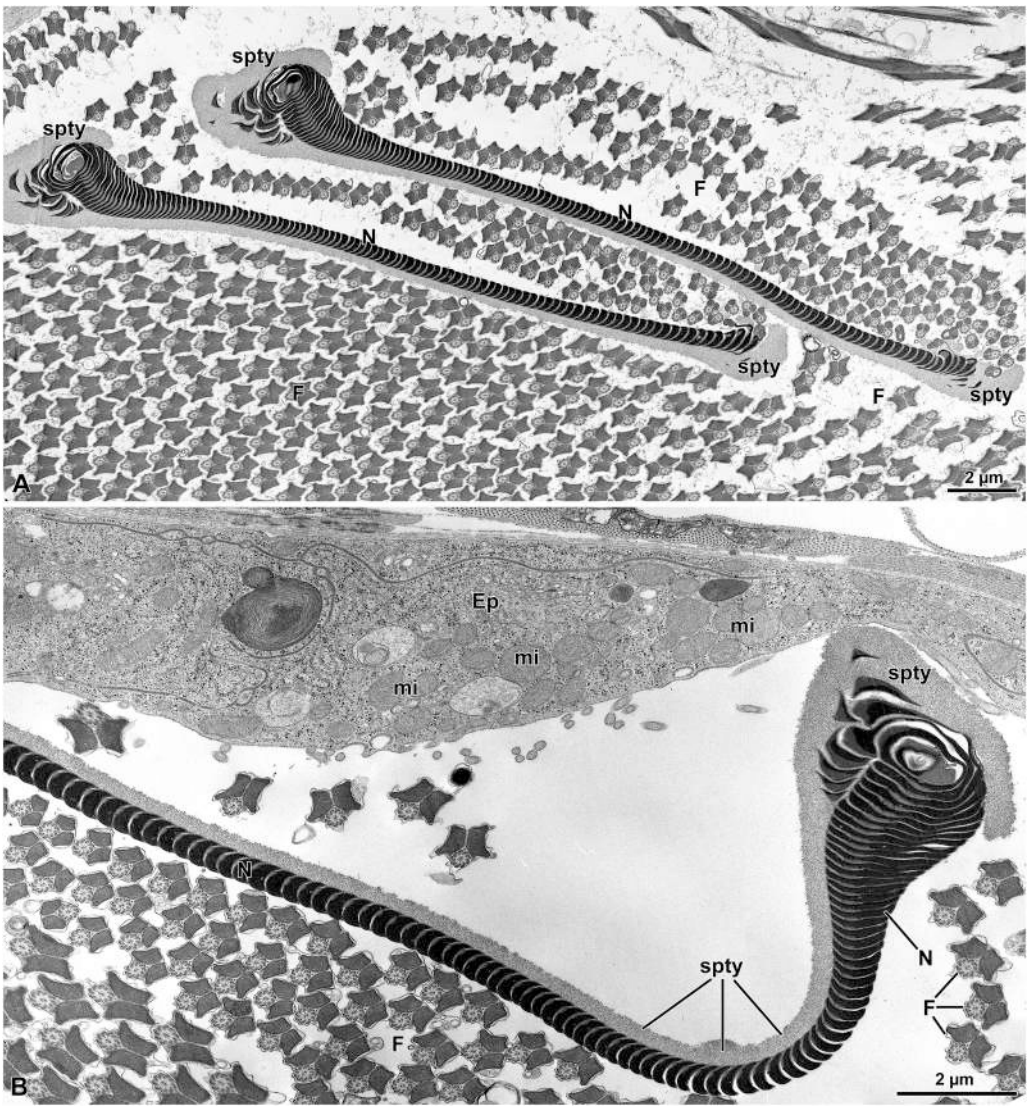

Fig. 5. S. optatus. A - Cross section through the deferent duct showing numerous sperm flagella and two long nuclear chains consisting of about hundred sperm heads, surrounded by a dense material, retained the spermatostyle. B - Detail of the long sperm-head chain to show the perfect insertion of nuclei in the chain. Note the material surrounding the sperm heads.
Ep, epithelium; F, flagella; mi, mitochondria; N, nuclei; spty, spermatostyle.

structure corresponds to a monolayered acrosome (Fig. 6E).

The peculiarity of the nuclear structure is its extremely long lateral region visible in cross-section, which bends on itself to form, when seen in longitudinal section, a kind of bell-shaped structure (Fig. 6B-C). All the sperm of the chains share this structure. The long chain of nuclei is maintained in a compact sequence by the perfect apposition of the several nuclear units and by the presence of a thick layer of fine granular electron-dense material, 0.85 µm thick, which form a sort of apical cup extending all along one side of the long nuclear chain and ending at the posterior extremity of it (Figs. 5A, B; 6A-D). This material is retained to be a spermatostyle.

Sperm head chains, without the material surrounding them, breaking into several parts are frequently present along the end of the deferent ducts (Fig. 6E). The end of the sperm lateral extension hosts the beginning of the flagellar axoneme (Fig. 7A-C). At this level a centriole is visible, surrounded by a scarse centriole adjunct material which also fills the axial region of the microtubular complex (Fig. 7A, B). The centriole doublets have no dynein arms but accessory tubules are visible at their periphery (Fig. 7A, B). Further, the complete flagellar structure, with a 9 + 9 + 2 axoneme and two ovoidal mitochondrial derivatives, becomes visible in cross-section. (Fig. 7B).

More distally, along the flagellum, the mitochondrial derivatives expand and take a quite unusual shape with their apical regions pointing outward in cross-sections (Fig. 7D-E). Mitochondrial matrix is electron-dense surrounded at the periphery by mitochondrial cristae (Fig. 7E). Two small accessory bodies looking like dense dots are present between the axoneme and the two mitochondrial derivatives.

The tail end is characterized by the size reduction of the mitochondrial derivatives and the loss of the integrity of the axoneme, which becomes a bundle of singlet microtubules.

3.2. *Scarodytes halensis*

3.2.1. *Male Genital system*

The male genital system of *Sc. halensis* consists of a pair of long unifollicular testes, folded at their half-length, about 5 mm long and 0.2–0.5 µm wide (Fig. 8A). A long deferent duct emerges at about half length of each testis (Fig. 8A, B). Deferent ducts are about 70 nm wide in cross-section and when stretched they reach up to 5 mm of length (Fig. 8B). They are often tightly folded and placed very close or contained within the end of testis.

3.2.2. *Spermatogenesis*

The testes contain a single follicle with germ cysts visible in semithin sections (Fig. 8C, D). When cross-sectioned, each cysts shows a cluster of 128 germ cells, as a result of 2^7 cell divisions occurring during spermatogenesis (Fig. 8D). During spermiogenesis, the spermatid nucleus has a large diameter (0.8 µm x 1.6 µm) in cross section and shows a

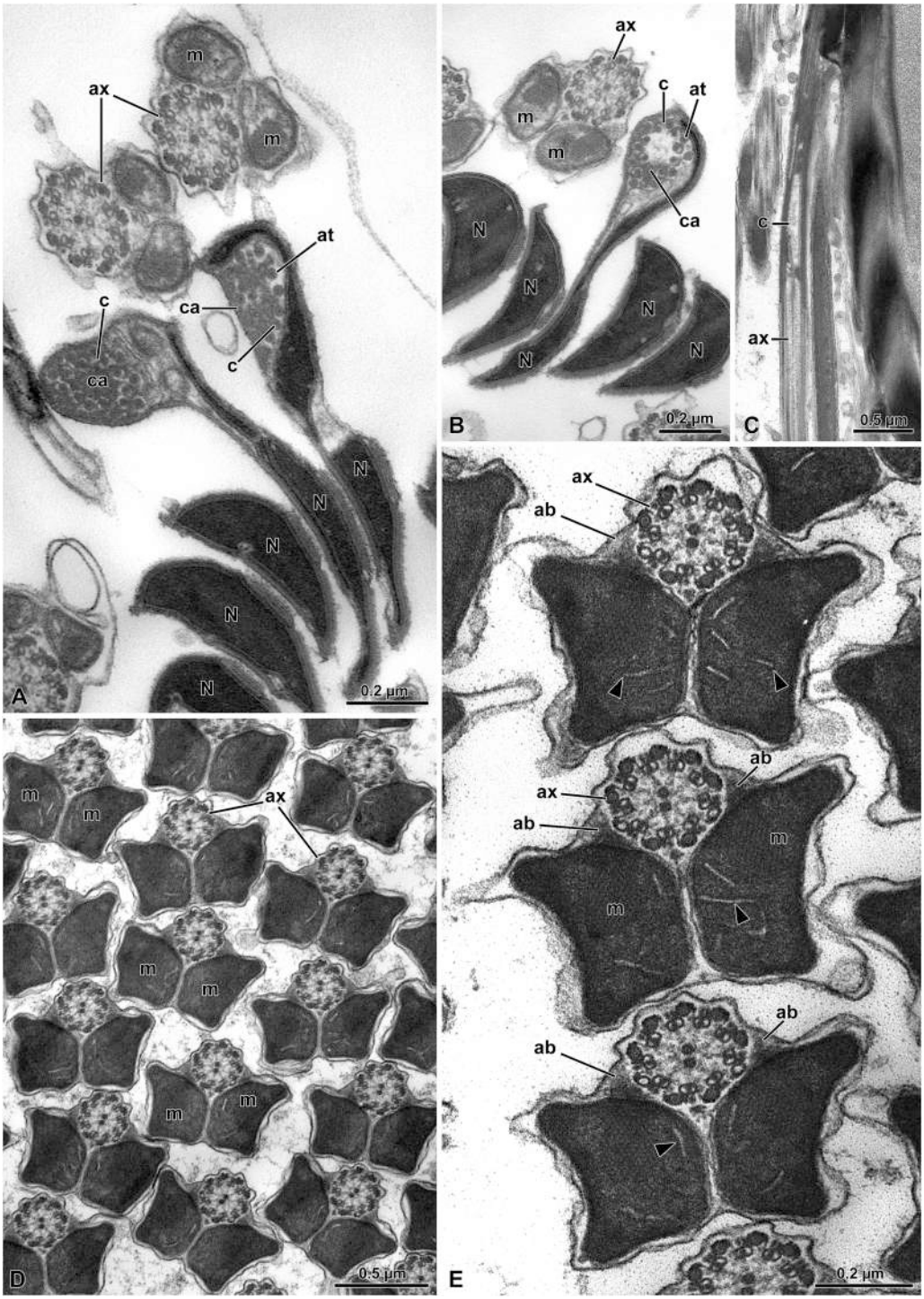

Fig. 7. S. optatus. A, B - Cross sections through the sperm-heads at the end of the nuclear chain showing the position of centriole, surrounded by the dense material of the centriole adjunct. Two sperm flagella, sectioned at the beginning of the axoneme, have ovoidal mitochondrial derivatives. C - Longitudinal section through the centriolar region and the axoneme. D, E - Cross sections through the sperm flagella with the peculiar shape of the mitochondrial derivatives. They show a dense matrix, into which cristae are still evident (arrowheads). Two small accessory bodies are visible in the upper region of mitochondrial derivatives.
ab, accessory bodies; at, accessory tubules; ax, axoneme; c, centriole; ca, centriole adjunct: m, mitochondrial derivatives; N, nucleus.

central cavity (about 0.46 µm in diameter) filled with flocculent material within which some microtubules are visible (Fig. 9A). The nuclear chromatin is compact and dense. All around the nucleus an orderly series of microtubules with short bridges contacting the nuclear envelope is visible (Fig. 9A, B). Only a short region (0.25 µm wide) is devoid of microtubules and hosts a short acrosome with a thin elliptic structure (Fig. 9B). In a later stage of spermiogenesis, the inner nuclear cavity progressively reduces its size and, at the same time, the thickness of the nucleus also decreases (Fig. 10A). The nucleus flattens around a groove with triangular shape (2.3 µm). The posterior region has, in cross-section, the shape of a thin bent cytoplasmic extension, 0.16 µm long and 60 nm thick, (Fig. 10A).

In the posterior nuclear region, a large dense globular body (0.9–1.2 µm wide) is present. This structure, possibly material of the centriole adjunct, is in contact with the centriolar region from which the flagellar axoneme starts (Fig. 9C-E).

In a final stage of spermatid maturation, the sperm nuclei are arranged in long series of orderly juxtaposed elements (Fig. 10B). An electron-dense material is visible between the sperm heads (Figs. 10B; 11G). The centriole is flanked by two slender mitochondrial derivatives, only 0.16 µm long in cross-section. (Fig. 9E).

The almost mature spermatids have typical flagellar axoneme with

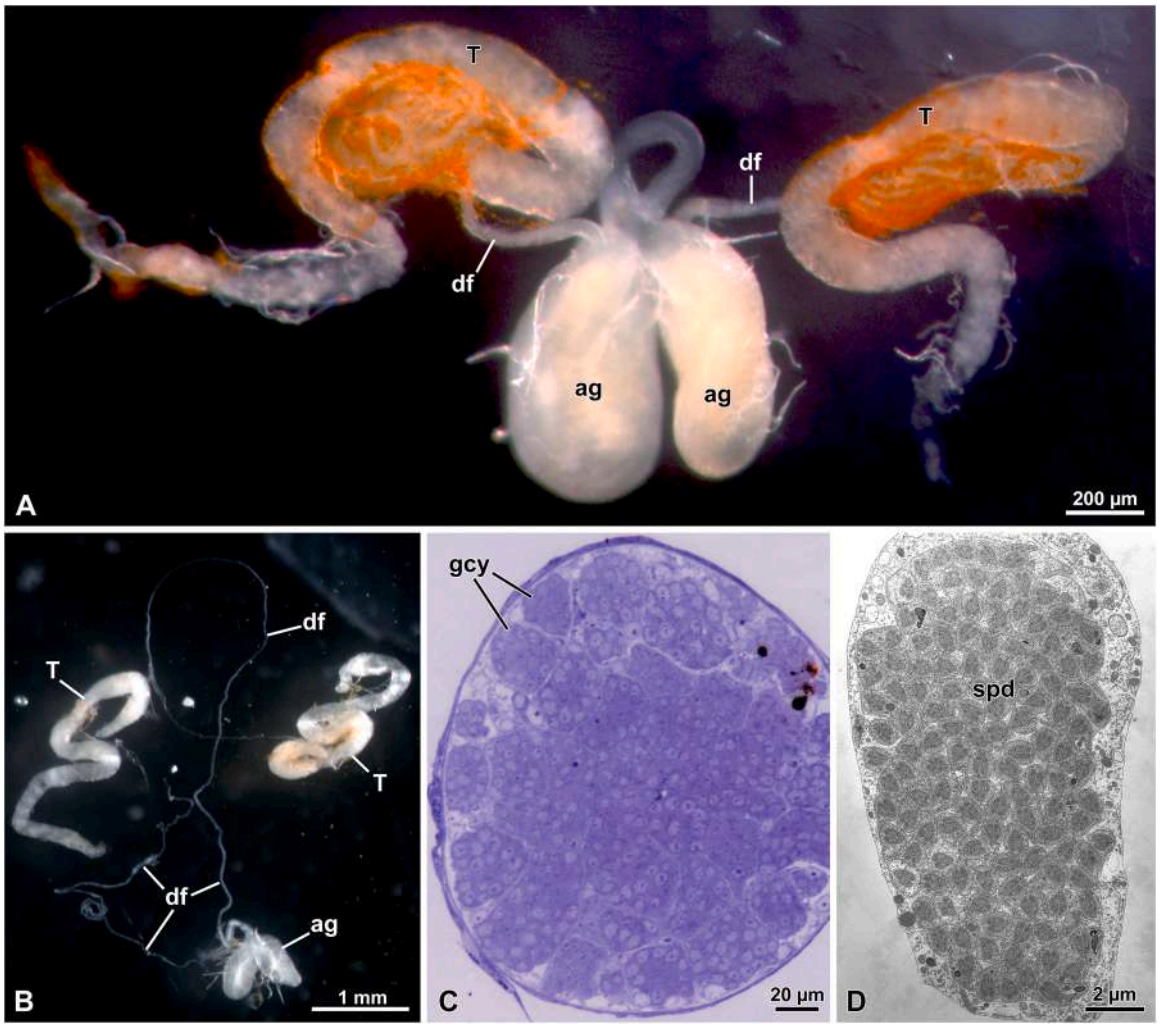

Fig. 8. Scarodytes halensis. A - Light microscopic view of the male genital apparatus with long cylindrical testes, deferent ducts and accessory gland. B - after stretching, the deferent ducts become very long. C - Semithin section of the monofollicular testis showing several cysts of germ cells. D - Cross section of a sperm cyst with numerous spermatids.
Ag, accessory glands; df, deferent ducts; gcy, germ cysts; spd, spermatids; T, testes.

$9 + 9 + 2$ microtubular complex and two elongated (0.5 µm) mitochondrial derivatives, in cross-section (Fig. 9E).

3.2.3. *Sperm ultrastructure*

The deferent duct epithelium has cells, 0.15–0.30 µm high, with elliptical nuclei 0.6 µm long and 0.16 µm wide. In the cytoplasm few mitochondria and some cisterns of rough endoplasmic reticulum are visible. Secretory material is very scarse, consisting in some dense vesicles (Fig. 12A).

The sperm are 0.615 mm long with a head about 12 µm long (Fig. 11A). The sperm head is quite peculiar as it shows a triangular shape forming a kind of groove (Fig. 11B, C). In cross-section the nuclei have the shape of a flattened dense ring with walls 0.17 µm thick. The posterior region is thinner and hosts the centriole. Two elliptical mitochondrial derivatives are present (Fig. 12B-F). Their matrix becomes dense, particularly in the region facing the axoneme. Two small accessory bodies are present on the side of mitochondrial derivatives close to the axoneme (Fig. 12B).

When the bundles of sperm move along the deferent duct, they form compact structures with orderly arranged nuclei (Fig. 11D-G). When the lumen of the deferent ducts becomes narrowed, it is not rare to find sperm flagella with mitochondrial derivatives becoming thin and elongated due to the compression of the adjacent sperm (Fig. 12B-E).

The flagellar axoneme ends with the reduction of the size of the mitochondrial derivatives up to their end. The axonemal tip has a bundle of singlet microtubules surrounded by a plasma membrane with a clearly visible fluffy glycocalyx (Fig. 12F).

4. Discussion

The sperm ultrastructure of *Stictonectes optatus* and *Scarodytes halensis* reported in this study represents the first available description of members of Dytiscidae-Hydroporinae. It is thus relevant and interesting to compare the results obtained on these species with those previously reported for other Dytiscidae and other Adephaga. (Mackie and Walker, 1974; Werner, 1976, 1983; Dallai and Afzelius, 1985; Carcupino et al., 2002; Sasakawa, 2007; Sasakawa and Toki, 2008; Hodgson et al., 2013; Schubert et al., 2017; Dallai et al., 2019, 2020; Gomez and Maddison, 2020; Salazar et al., 2022; Gomez et al., 2023).

As to the morphology of the male genital system, both species have unifollicular testes, and those of *S. optatus* have a globular shape. Moreover, this species displays very large accessory glands, while those of *Sc. halensis* are smaller. It is possible that *S. optatus* glands are involved in the production of a mating plug during *S. optatus* mating (Dallai, pers. obs.).

It is reasonable to assume that the different organization of the

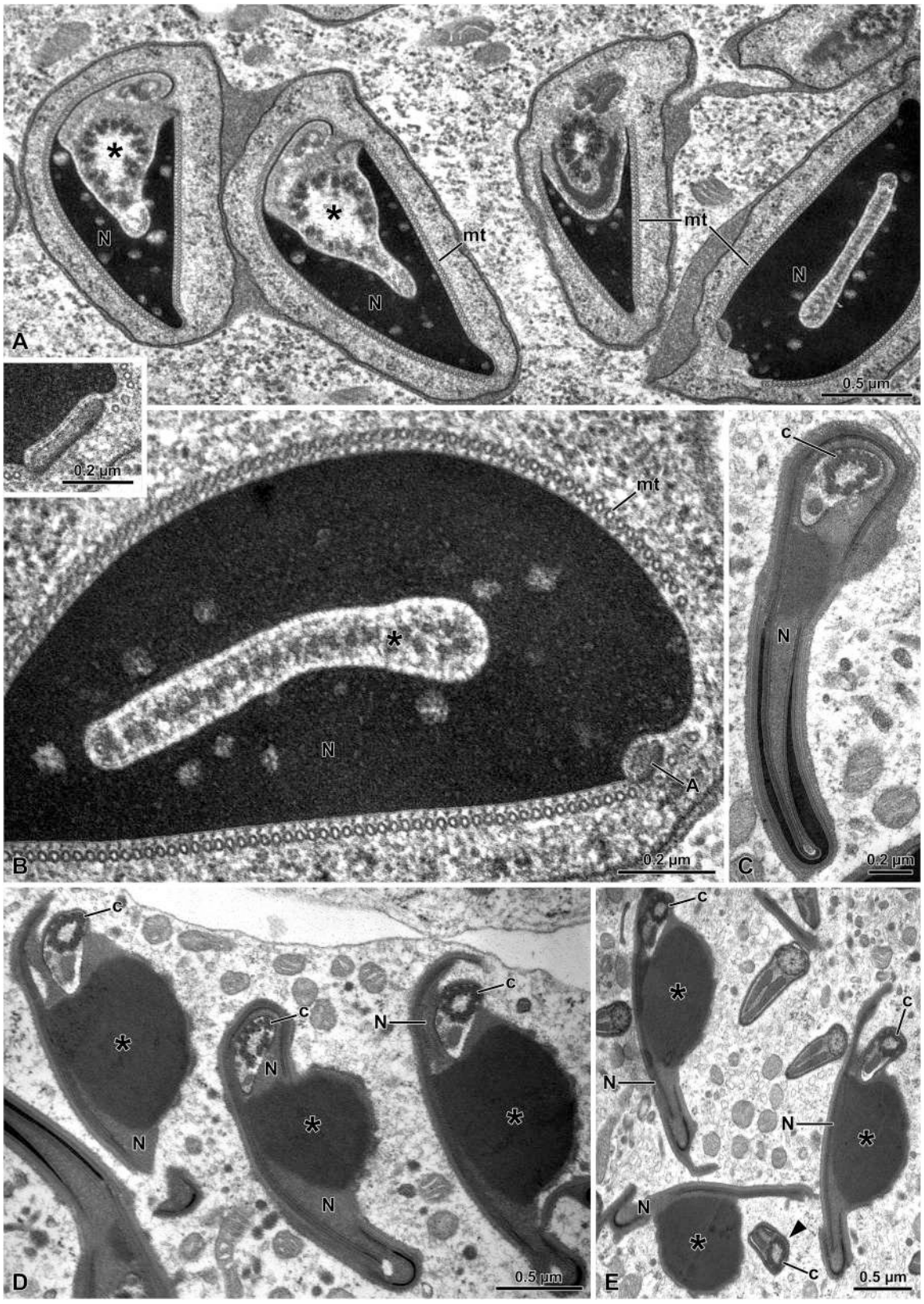

Fig. 9. Sc. halensis. A - Cross section of aged spermatid nuclei hosting in their central region flocculent material and some microtubules (asterisks). A layer of microtubules surrounds the structures. B - High magnification of a cross section of the anterior nuclear region, showing the inner part with flocculent material and microtubules. At one nuclear extremity, a small acrosome is visible. Note the orderly series of microtubules surrounding the nucleus taking contact with the nuclear envelope by short bridges. In the inset, the small flattened acrosome is visible at the nuclear extremity. C - Detail of the laminar nucleus hosting the centriole. D, E - Cross sections of the posterior nuclear region of almost mature spermatids. Note the centriole and the electron-dense ball present at this level (asterisk). A centriole with two mitochondrial derivatives (arrowhead) is also visible.
A, acrosome; c, centriole; mt, microtubules; N, nuclei.

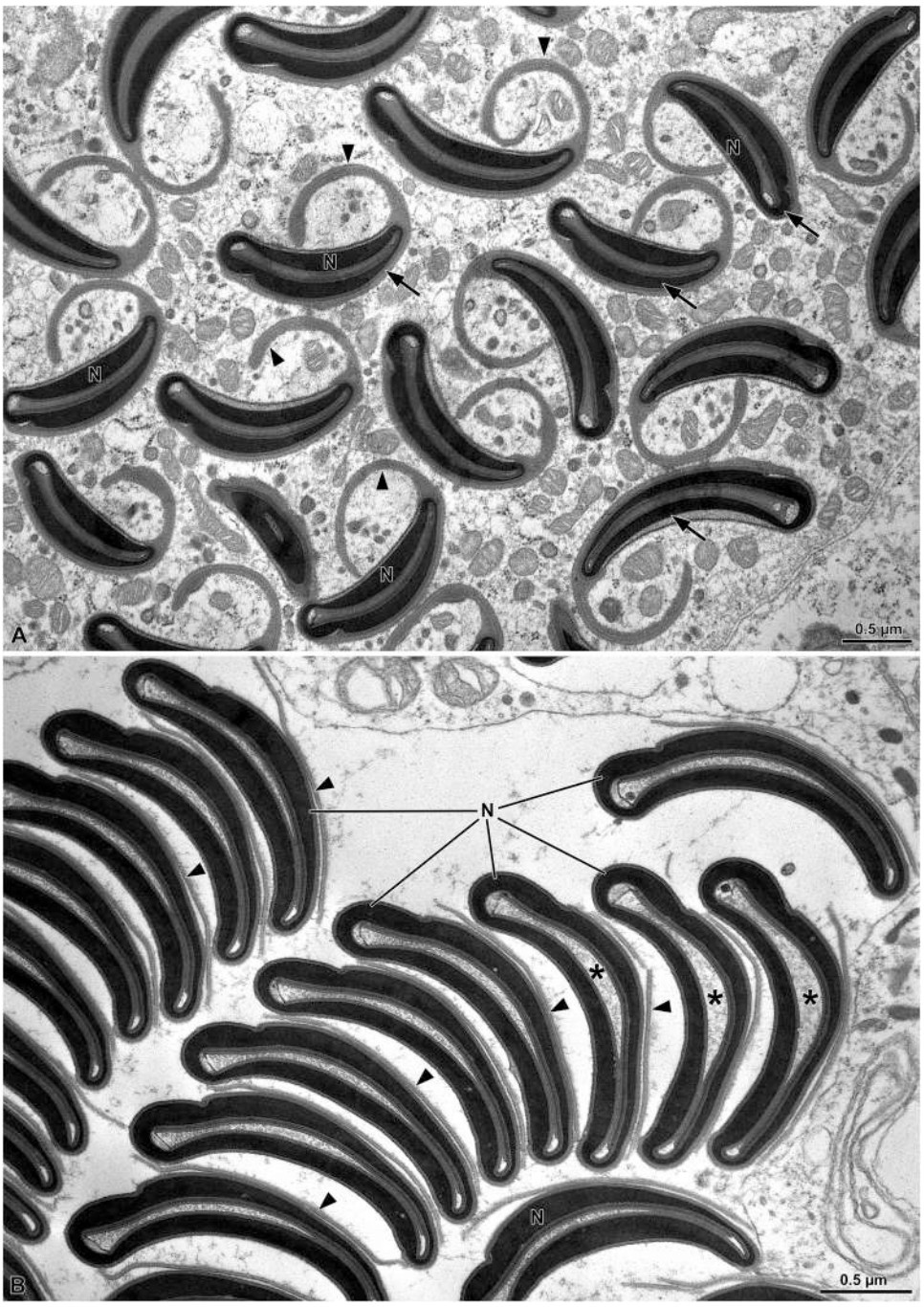

Fig. 10. Sc. halensis. A - Cross section of spermatid in the testes. Nuclei show their peculiar shape with an anterior thick (arrows) and a posterior bent laminar regions (arrowheads) containing a thin layer of cytoplasm. B - Cross section through the deferent duct. The mature flattened nuclear rings are orderly arranged in chains. Note the material in the inner nuclei (asterisks) and the filamentous material between the sperm (arrowheads).
N, nuclei.

genital organs in the two species.

depends on a different strategy for a reproductive success. Moreover, this difference could be responsible for the different modality to organize the sperm bundle. In *Sc. halensis* the sperm heads, in the deferent duct, form regularly arranged stacks were the tip of the sperm head slips into the hollow portion of the neighboring sperm head, maintained in situ only by their perfect apposition and some internuclear material, as occurs in the so called sperm rouleaux. On the contrary, in *Stictonectes optatus* the sperm-heads stick together to form long stacks which are surrounded by a quite evident layer of secretory material.

Considering this difference between the species, we could give to the secretion surrounding the head stacks of *S. optatus* the significance of a spermatostyle. The difference between the two species here studied becomes relevant when considering that, whilst the spermatostyle was so far identified only in the terrestrial Carabidae and the aquatic Gyrinidae, the other aquatic "Hydradephaga" species, on the contrary, have other mechanisms of sperm aggregation (Salazar et al., 2022). However, it is worth mentioning that a small mass of fluffy material, similar to that observed in *S. optatus,* was described in the most apical sperm pair of *Hydaticus seminiger* (Dallai and Afzelius, 1985) and in *H. transversalis* (Werner, 1976).

The morphology and the length of the spermatostyle are pretty variable among Carabidae (Dallai et al., 2019, 2020; Hodgson et al., 2013; Sasakawa, 2007; Schubert et al., 2017) and Gyrinidae (Salazar et al., 2022) and can be useful to distinguish the taxa (Salazar et al., 2022) in addition to the external morphology of the species.

As mentioned by Schubert et al. (2017), the spermatostyle of the carabid *Limodromus assimilis* contains glycoproteins, and an analogous chemical composition was found in the diving beetles *Dytiscus marginalis* and *Colymbetes fuscus* studied by Mackie and Walker (1974). This

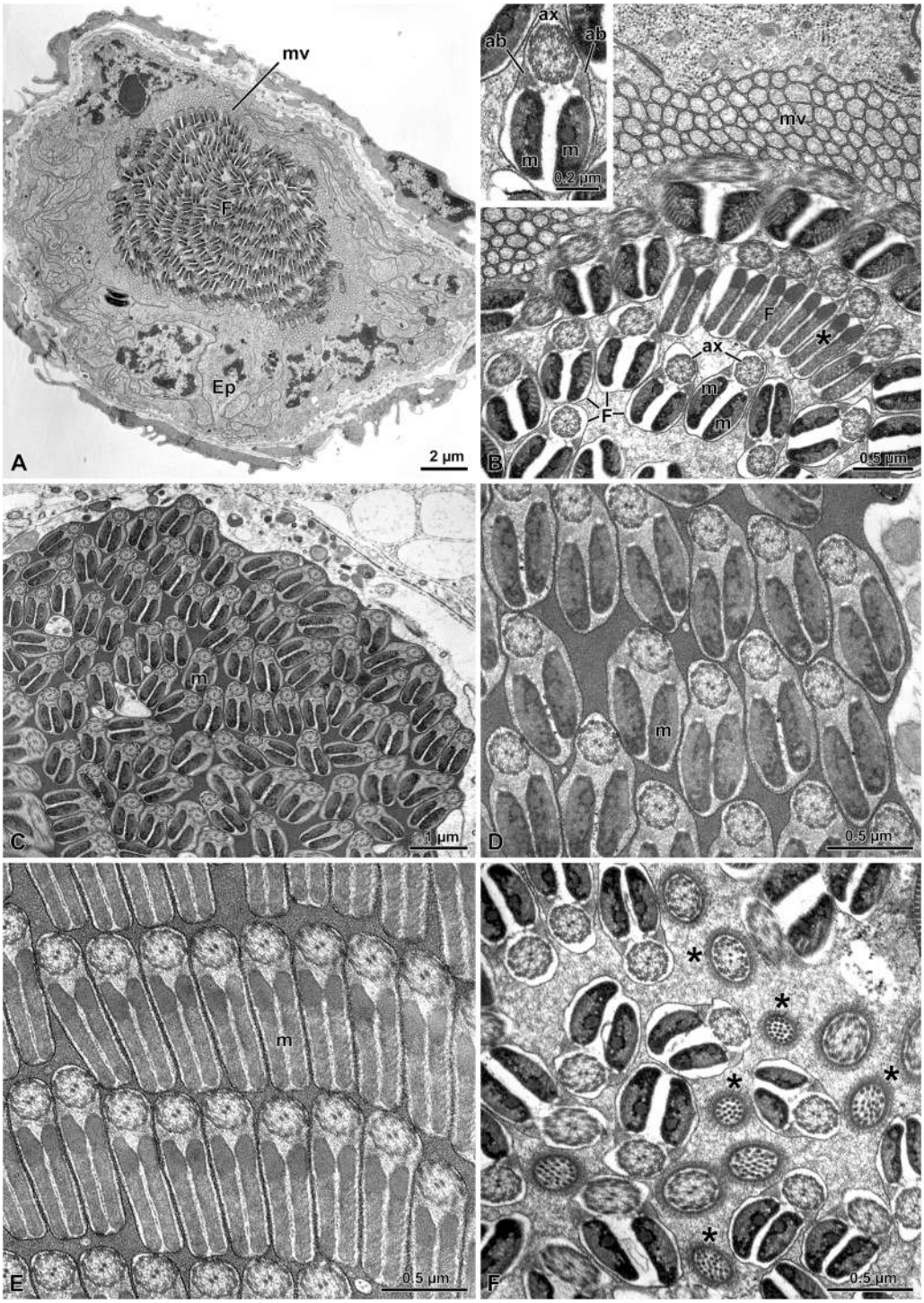

Fig. 12. Sc. halensis. A. Cross section through a deferent duct epithelium with the lumen filled with sperm flagella adhering to microvilli. B - Detail of the previous figure to show the general shape of sperm flagella, with the axoneme, the small accessory bodies, and the mitochondrial derivatives. When pressed these latter, become thin and long (asterisk). In the inset, detail of a sperm flagellum. C, D, E - Sperm bundles with mitochondrial derivatives showing different shapes depending from the available space in the deferent lumen. F - Cross section of the deferent duct with the flagellar ends (asterisk) showing a fluffy glycocalyx.
ab, accessory bodies; ax, axoneme; F, flagella; m, mitochondrial derivatives; mv, microvilli.

structure, in the gyrinid genus *Gyretes,* contains a combination of protein and carbohydrates (Salazar et al., 2022). It is presumable that, considering the poor electron-density of the structure and the scarce presence of rough endoplasmic reticulum and some Golgi apparatuses in the deferent duct epithelial cells, the spermatostyle of *S. optatus* could also contain a similar chemical composition. On the other hand, in different insects, Hayashi (1997) found a complex of proteins and polysaccharides in the structures protecting the sperm bundles integrity.

Taking into account the sperm length of the two species, they belong to those Adephaga characterized by median or larger length of sperm (Ballowitz, 1895; Mackie and Walker, 1974; Werner, 1976; Dallai and Afzelius, 1985, 1987; Higginson et al., 2012), but this sperm parameter is quite variable within the group. On the contrary, the structure of the several sperm components is of importance to a comparative analysis with other members of Adephaga (Dallai et al., 2019, 2020; Salazar et al., 2022; Gomez et al., 2023).

The presence of different models of sperm aggregations is a common event among Dytiscidae. As well described by Higginson et al. (2012), sperm aggregation was found to be the ancestral condition and a similar condition was evident in the Carabidae and Gyrinidae (Carcupino et al., 2002; Sasakawa, 2007: Schubert et al., 2017; Hodgson et al., 2013; Dallai et al., 2019, 2020; Gomez and Maddison, 2020; Salazar et al.,

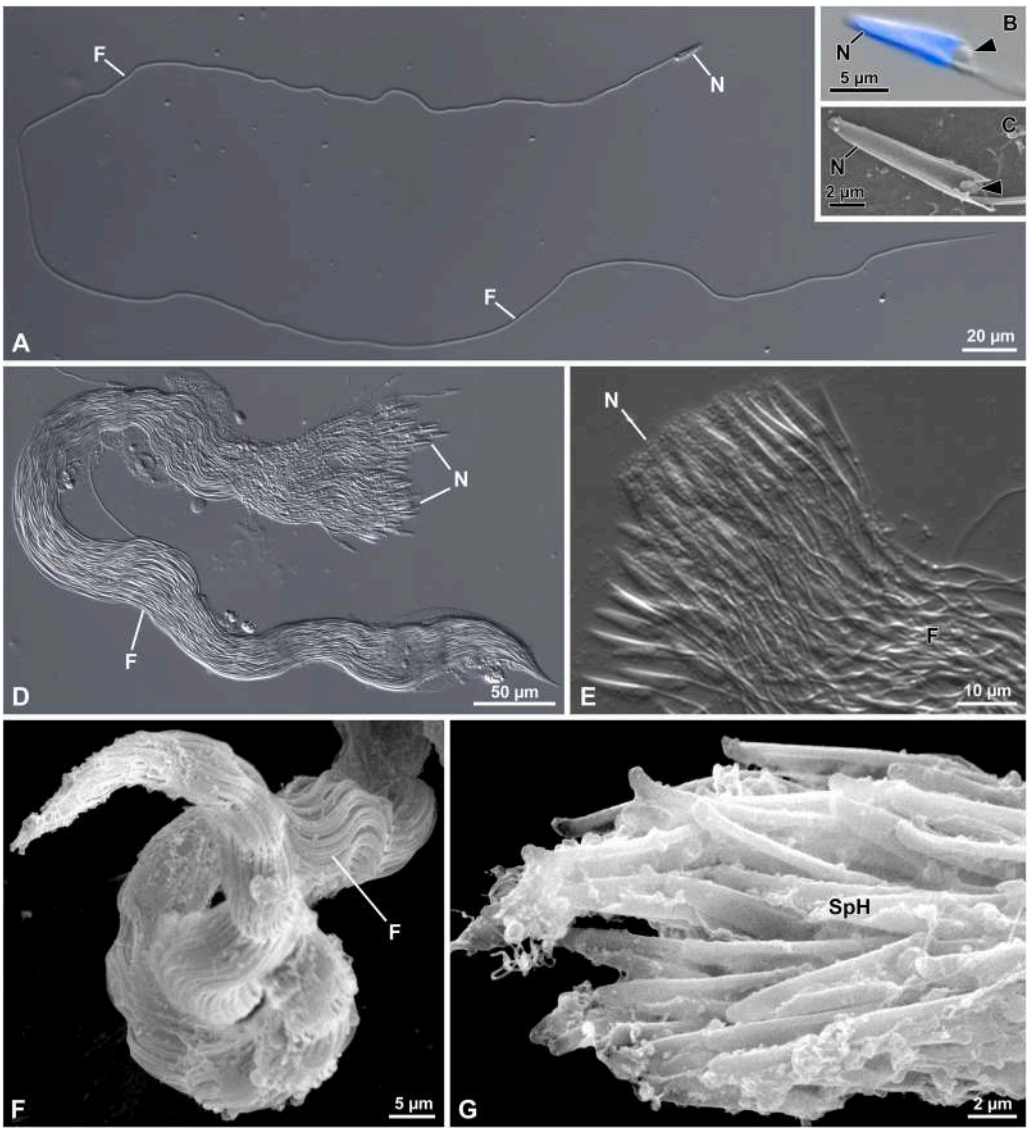

Fig. 11. Sc. halensis. A - Light microscopic view of a free sperm from deferent duct. B - Fluorescent sperm nucleus after Hoechst staining. Note the triangular groove shape of the nucleus, with a ball structure at its posterior end (arrowhead). C - The same as in B after Scanning electron microscopy. D - A sperm bundle taken from the deferent duct at the interference light microscope. E - Sperm bundle showing the anterior nuclear region. F, G - Two sperm bundles at the Scanning electron microscopy, showing the flagellar and the nuclear regions, respectively. Note the presence of some residual material between the nuclei.
F, flagella; N, nuclei; SpH, sperm heads.

2022; Gomez et al., 2023).

The ultrastructure of the several sperm components of the two species also deserves some considerations. The acrosome is quite similar in both the species as a thin structure adherent to the apical surface of the nucleus. Such sperm feature is shared by other members of Dytiscidae (Werner, 1976; Mackie and Walker, 1974; Dallai and Afzelius, 1985, 1987). The nucleus is flat and large in both the species, with the laminar posterior region hosting the centriole. From this structure a long axoneme starts and prolongs up to the tail end. No material is present cementing the flagella which can consequently freely swim. The centriole is embedded in the centriole adjunct material. In *Sc. halensis*, a globular mass of dense material, possibly of residual cytoplasm, marks the nuclear posterior region. The flagellar axoneme of both species has the conventional $9 + 9 + 2$ microtubular pattern of insects, with peripheral dense accessory tubules as also are the two central tubules. Scanty dense material forming the small accessory bodies is stored between the axoneme and the two mitochondrial derivatives. The size reduction of the accessory bodies is the consequence of the reduced amount of centriole adjunct material surrounding the centriole located beneath the nucleus. This feature is also shared by Adephaga beetles, such as species of Dytiscidae, Carabidae and Gyrinidae (Werner, 1976; Mackie and Walker, 1974; Dallai and Afzelius, 1985, 1987; Jamieson et al., 1989; Dallai et al., 2016, 2019; Gomez and Maddison, 2020; Salazar et al., 2022; Gomez et al., 2023) and is related to the well-known connection between the centriole adjunct material and the accessory bodies (Dallai, 2014; Jamieson et al., 1989).

The mitochondrial derivatives have a quite different shape in the two species making easy to distinguish them. In *Sc. halensis* they are elliptic kidney-shaped in cross-section and when the sperm are strictly associated in some regions of the deferent ducts, they become thin and elongated. In *S. optatus* the mitochondrial derivatives have a peculiar shape, somewhat recalling, in cross-section, the stylized men by Keith Haring, with their outward protruding apical region. The mitochondrial matrix is homogeneously dense and cristae are visible within it.

In both the species the tail tip shows a reduction of the flagellar axoneme to a complex of singlet microtubules. Interestingly, at this level in the *Sc. halensis* sperm tail, a fuzzy material is visible around the plasma membrane, recalling what was described in some curculionids beetles (Dallai et al., 1998).

The different organization of the sperm-head stacks in the two species here treated has a further consequence in the female spermatheca at mating (Dallai, pers. obs.). Sperm-head stacks of *S. optatus* can be partly dissociated in the last tracts of the deferent ducts, but some of them, even if having lost the spermatostyle, remain grouped in the spermatheca without evident changes, becoming free sperm only in the fertilization duct (pers. observ.). This is not the case of *Sc. halensis*. As to the

origin of the two above described different types of aggregation, it is difficult to consider them as simple mechanisms for the precise head alignment which would be able to be interchanged between the two species. Such a situation was mentioned by Higginson et al. (2012) in *Rhantus* sp. (Colymbetinae), where sperm form typical aggregates that, after transfer to the female, change their appearance acquiring a different model of aggregation. This is not the case for *Sc. halensis* and *S. optatus*. We are inclined to think that this difference is due to a different origin of sperm aggregation in these diving beetles and in particular to the lack of a spermatostyle around the sperm head stacks of *Sc. halensis*.

Observations on the ultrastructure of the deferent duct epithelium confirm such our opinion. *S. optatus* has epithelial cells rich of secretory material, discharged in the deferent lumen, while those of *Sc. halensis* do not. It is known that the extracellular material constituting the spermatostyle is produced by the epithelial cells of the deferent duct (Carcupino et al., 2002; Hodgson et al., 2013; Schubert et al., 2017).

The possibility that a selective environmental factor could have a role in this contest seems to be very improbable considering that the two species live in the same pond. It is instead possible that the sperm aggregation may depend on the quite different organization of their female genital apparatuses and to a notable difference in the type of sperm transfer to the female (Dallai pers. obs.). This conclusion is also supported by an interpretation by Miller (2001): "The Hydroporinae take on a variety of general forms as to the female genital system organization. The taxa have extensive and complicated differences in bursal and spermathecal shape, length and diameter of the fertilization and spermathecal ducts".

The functional significance of sperm conjugation was explained in different way. It was demonstrated that sperm bundles often have a greater velocity than isolated sperm cells (Bawa, 1964; Hayashi, 1998; Higginson and Pitnick, 2011; Dallai et al., 2019, 2020; Salazar et al., 2022), and this is a significant advantage for cells involved in fertilization. Moreover, the sperm bundles may offer a physiological protection against environmental factors (Phillips, 1970) or improve egg penetration (Hayashi, 1998). The most obvious explanation, however, is that sperm conjugation facilitates sperm transfer and increases the amount of sperm transferred to the female at mating. This could indeed enhance the reproductive efficiency, avoiding remating of female with a second male (Pitnick, 1996; Higginson and Pitnick, 2011).

A final consideration comes from the evidence that the long sperm-head chains of *S. optatus* can often break along their transit through the deferent ducts. We cannot rule out the possibility that the reaggregation of the single parts in new long structures, which we have observed in the female spermatheca (Dallai pers. obs.), can occur with the same components and in the same order, regenerating the same original sperm bundle. In the alternative, however, the new bundles could be rearranged by secondary aggregation of sperm from different chains, thereby increasing the genetic variability of the ejaculate.

In conclusion, the spermatostyle of *S. optatus* described here represents the first record of a structural specialization to keep sperm-heads grouped together in the Dytiscidae. Further studies on other diving beetles are needed to establish whether the new evidence described here represents an isolated case or, instead, such specialization is shared by other members of the group. As suggested by Higginson et al. (2012), ancestral state reconstruction supports the presence of sperm conjugation in the ancestor of diving beetles, which has subsequently been lost at multiple times throughout the lineage of Adephaga. Thus, the possibility of a degree of homoplasy of the types of sperm aggregation described in Adephaga cannot be ruled out. Future studies will allow to give an answer to this significant question.

Declaration of Competing Interest

The authors declare that they have no known competing financial interests or personal relationships that could have appeared to influence the work reported in this paper.

Data availability

No data was used for the research described in the article.

Acknowledgments

The Authors are grateful to Dr Saverio Rocchi for the identification of the specimens of diving beetles studied in the present work, and for the useful information about the systematic position of these species.

References

Ballowitz, E., 1895. Die dopple Spermatozoen der Dytisciden. Z. für Wiss. Zool. 60, 458–499.
Bawa, S.R., 1964. Electron microscope study of spermiogenesis in a fire-brat insect, Thermobia domestica Pack. J. Cell Biol. 23, 431–445.
Beutel, R.G., Ribera, I., Fikáček, M., Vasilikopoulos, A., Misof, B., Balke, M., 2020. The morphological evolution of the Adephaga (Coleoptera). Syst. Entomol. 45, 378–395.
Birkhead, T.R., 2000. Defining and demonstrating postcopulatory female choice—again. Evolution 54, 1057–1060.
Breland, O.P., Simmons, E., 1970. Preliminary studies of the spermatozoa and the male reproductive system of some whirligig beetles (Coleoptera: Gyrinidae). Entomol. N. 81, 101–110.
Carcupino, M., Stocchino, A.G., Corso, G., Manca, I., Casale, A., 2002. Morphology of the male reproductive apparatus and spermatodesms formation in *Percus strictus strictus* (Coleoptera, Carabidae). In: van der Horst, G., Franken, D., Bornman, R., Bornman, T., Dyer, S. (Eds.), Proceedings of 9th International Symposium on Spermatology. Bologna, Monduzzi Editore, pp. 31–34.
Dallai, R., 2014. Overview on spermatogenesis and sperm structure of Hexapoda. Arthropod Struct. Dev. 43, 257–290.
Dallai, R., Afzelius, B.A., 1985. Membrane specializations in the paired spermatozoa of dytiscid water beetles. Tissue Cell 17, 561–572.
Dallai, R., Afzelius, B.A., 1987. Sperm ultrastructure in the water beetles (Insecta, Coleoptera). Boll. di Zool. 54, 301–306.
Dallai, R., Afzelius, B.A., Lupetti, P., Osella, G., 1998. Sperm structure of some Curculionoidea and their relationship with Chrysomeloidea. Mus. Reg. Sci. Nat. Torino 27–50.
Dallai, R., Paoli, F., Mercati, D., Lupetti, P., 2016. The centriole adjunct of insects: need to update the definition. Tissue Cell 48, 104–113.
Dallai, R., Mercati, D., Giglio, A., Lupetti, P., 2019. Sperm ultrastructure in several species of Carabidae beetles (Insecta, Adephaga) and their organization in spermatozeugmata. Arthropod Struct. Dev. 51, 1–13.
Dallai, R., Mercati, D., Fanciulli, P.P., Petrioli, A., Lupetti, P., 2020. New findings on the sperm ultrastructure of Carabidae (Insecta, Coleoptera). Arthropod Struct. Dev. 54, 100912.
Gomez, R.A., Maddison, D.R., 2020. Novelty and emergent patterns in sperm: Morphological diversity and evolution of spermatozoa and sperm conjugation in ground beetles (Coleoptera: Carabidae). J. Morphol. 8, 862–892.
Gomez, R.A., Mercati, D., Lupetti, P., Fanciulli, P.P., Dallai, R., 2023. Morphology of male and female reproductive systems in the ground beetle *Apotomus* and the peculiar sperm ultrastructure of *A. rufus* (P. Rossi, 1790) (Coleoptera, Carabidae). Arthropod Struct. Dev. 72, 101217 https://doi.org/10.1016/j.asd.2022.101217 (Epub ahead of print).
Hayashi, F., 1997. A trypsin-degradable protein agglutinates fish fly sperm-bundles. Int. J. Insect Morph. Physiol. 26, 63–66.
Hayashi, F., 1998. Sperm co-operation in the fish fly, *Parachauliodes japonicus*. Funct. Ecol. 12, 347–350.
Higginson, D.M., Pitnick, S., 2011. Evolution of intra-ejaculate sperm interactions: do sperm cooperate? Biol. Rev. 87, 249–270.
Higginson, D.M., Miller, K.B., Segraves, K.A., Pitnick, S., 2012. Convergence, recurrence and diversification of complex sperm traits in diving beetles (Dytiscidae). Evolution 66 (5), 1650–1661.
Hodgson, A.N., Ferenz, H.-J., Schneider, S., 2013. Formation of sperm bundles in *Pterostichus nigrita* (Coleoptera: Carabidae). Invertebr. Reprod. Dev. 57, 120–131.
Jamieson, B.G.M., Dallai, R., Afzelius, B.A., 1999, Insects. Their Spermatozoa and Phylogeny IBH Publishing Ltd., Oxford, p. 554.
Mackie, J.B., Walker, M.H., 1974. A study of the conjugate sperm of the dytiscid water beetles *Dytiscus marginalis* and *Colymbetes fuscus*. Cell Tissue Res 148, 505–519.
Miller, G.T., Pitnick, S., 2002. Sperm-female coevolution in *Drosophila*. Science 298, 1230–1233.
Miller, K.B., 2001. On the phylogeny of the Dytiscidae (Insecta: Coleoptera) with emphasis on the morphology of the female reproductive system. Insect Syst. Evol. 32 (1), 45–89.
Miller, K.B., 2003. The phylogeny of diving beetles (Coleoptera: Dytiscidae) and the evolution of sexual conflict. Biol. J. Linn. Soc. 79, 359–388.
Miller, K.B., Bergsten, J., 2016. Diving beetles of the world. Systematics and Biology of the Dytiscidae. John Hopkins University press,, Baltimore, p. 320.
Nilsson, A.N., 2001, World catalogue of insects. Vol. 3. Dytiscidae Coleoptera. Stenstrup: Apollo Books, 395 p.

Nilsson, A.N., Fery, H., 2006. World Catalogue of Dytiscidae - corrections and additions, 3 (Coleoptera: Dytiscidae). Koleopterol. Rundsch. 76, 55–74.
Phillips, D.M., 1970. Insect sperm: their structure and morphogenesis. J. Cell Biol. 44 (2), 243–277.
Pitnick, S., 1996. Investment in testes and the cost of making long sperm in *Drosophila*. Am. Nat. 148, 57–90.
Pitnick, S., Hosken, D.J., Birkhead, T.R., 2009. Sperm morphological diversity. In: Birkhead., T.R., Hosken., D.J., Pitnick, S. (Eds.), Sperm Biology, an Evolutionary Perspective. Academic Press, San Diego, CA, pp. 69–149.
Pizzari, T., Parker, G.A., 2009. Sperm competition and sperm phenotype. In: Birkhead., T.R., Hosken., D.J., Pitnick, S. (Eds.), Sperm Biology, an Evolutionary Perspective. Elsevier, London, pp. 205–244.
Salazar, K., Novais, A., Lino-Neto, J.L., Serrão, J.E., 2022. The sperm aggregation in a whirligig beetle (Coleoptera, Gyrinidae): structure, functions, and comparison with related taxa. Org. Divers. Evol. 22, 355–375.
Sasakawa, K., 2007. Sperm bundle and reproductive organs of carabid beetles tribe Pterostichini (Coleoptera: Carabidae). Naturwissenschaften 94, 384–391.
Sasakawa, K., Toki, W., 2008. A new record, sperm bundle morphology and preliminary data on the breeding type of the ground beetle *Jujiroa estriata* Sasakawa (Coleoptera: Carabidae: Platynini). Èntomol. Sci. 11, 415–417.
Schubert, L.F., Krüger, S., Moritz, G.B., Schubert, V., 2017. Male reproductive system and spermatogenesis of *Limodromus assimilis* (Paykull 1790). PloS One 12 (7), e0180492.
Stockley, P., Gage, M.J.G., Parker, G.A., Møller, A.P., 1997. Sperm competition in fishes: the evolution of testis size and ejaculate characteristics. Am. Nat. 149, 933–954.
Werner, G., 1976. Entwicklung und Bau der Doppel Spermien bei den Dytisciden *Acilius sulcatus* L., *Dytiscus marginalis* L. und *Hydaticus transversalis* Pont. (Coleoptera). Zoomorphologie 83, 49–87.
Werner, G., 1983. The joint spermatozoa of Dytiscidae. 4th Int. Symp. . Spermatol. 1982, 167–170.